Journal of Materials Chemistry C

Tetraphenylethene-Decorated Carbazoles: Synthesis, Aggregation-Induced Emission, Photo-Oxidation and Electroluminescence

Journal:	*Journal of Materials Chemistry C*
Manuscript ID:	TC-ART-05-2014-001019.R1
Article Type:	Paper
Date Submitted by the Author:	03-Jun-2014
Complete List of Authors:	Gong, Wen-Liang; Huazhong University of Science and Technology, Wang, Bo; Huazhong University of Science and Technology,, Aldred, Matthew; Huazhong University of Science and Technology, Li, Chong; Huazhong University of Science and Technology, Zhang, Guo-Feng; Huazhong University of Science and Technology, Chen, Tao; Huazhong University of Science and Technology, Wang, Lei; Huazhong University of Science and Technology, Wuhan National Laboratory for Optoelectronics; Zhu, Ming-Qiang; Huazhong University of Science and Technology, Wuhan National Laboratory for Optoelectronics

Journal Name

RSCPublishing

ARTICLE

Tetraphenylethene-Decorated Carbazoles: Synthesis, Aggregation-Induced Emission, Photo-Oxidation and Electroluminescence

Cite this: DOI: 10.1039/x0xx00000x

Received 00th January 2012,
Accepted 00th January 2012

DOI: 10.1039/x0xx00000x

www.rsc.org/

Wen-Liang Gong, Bo Wang, Matthew. P. Aldred,* Chong Li, Guo-Feng Zhang, Tao Chen, Lei Wang and Ming-Qiang Zhu*

In this paper, the bromination of carbazole has been controlled and then the subsequent mono, di, tri and tetra-bromocarbazoles have been subjected to Suzuki cross-coupling to yield a series of carbazole-tetraphenylethene (TPE) materials with varying the number of peripheral TPE groups. Accompanied with 2, 7-dibromo-carbazole, five new Cz-TPE materials are successfully synthesized. All the Cz-TPEs are non-fluorescent in THF and emit strong blue-green fluorescence in aggregate state (f_w = 90%) and thin films because of their aggregation induced emission (AIE) nature. In THF (10^{-5} M) solution, all the Cz-TPEs emit deep blue fluorescence after UV irradiation and we find that the more TPE groups, the slower the fluorescence enhances. In thin film (40 nm), the emission maximum blue shift, decreases and finally becomes non-emissive after about 1.5 h of UV irradiation for all the Cz-TPEs. We suppose these optical properties are attributed to the photo induced irreversible changes of TPE to diphenylphenanthrene derivatives. The photo-oxidation process for Cz-1TPE has been investigated and proved by HPLC analysis, ^{1}H NMR and LS-MS. The electrochemical properties of all the Cz-TPEs are investigate by cyclic voltammetry and accomplished with UV-absorption spectra, their energy levels are calculated. Finally, we applied the Cz-TPEs to organic light emitting diode (OLED) devices by spin coating deposition process with OLED devices configuration: ITO/PEDOT (40 nm)/Cz-TPEs (50 nm)/TPBi (40 nm)/LiF (1 nm)/Al (100 nm). All the EL devices emit blue-green light with a maximum luminance (L_{max}) of 2858, 1353, 986, 2088 and 1129 cd m^{-2}, a maximum current efficiency ($\eta_{c,max}$) of 3.5, 4.9, 3.1, 3.1 and 5.5 cd A^{-1}, a maximum power efficiency ($\eta_{P,max}$) of 2.1, 3.9, 2.2, 1.8 and 3.1 lm W^{-1} and turn on voltage (V_{on}) 3.5, 3.5, 3.3, 3.6 and 4.2 V, for Cz-1TPE, Cz-2TPE, Cz-3TPE, Cz-4TPE, Cz-2TPE (2, 7), respectively.

Introduction

Carbazole-based materials have been important within organic semiconductor research for several decades due to their efficient hole-mobility properties. As a result they have found widespread use in academic and commercial settings in areas such as organic light emitting diodes (OLEDs),[1] xerography[2] and solar cells.[3] With respect to OLEDs carbazole-based materials have been used as hole-transporting materials and incorporated into the light-emitting material to improve both hole-transporting and injection properties.[4] Current research regarding host materials for phosphorescence OLEDs has involved carbazole due to its high triplet energy level and low oxidation potentials.[5] In most cases carbazole materials for OLED applications are functionalized either at the 2, 7-, 3, 6- or the 9-(*N*) position.[6] However, we recently reported novel methods for the bromination of carbazole at the 1, 3, 6- and 1, 3, 6, 8- positions and subsequent Suzuki cross-couplings afforded new carbazole oligomeric materials.[7a]

Recently great progress has been made regarding materials that display aggregation induced emission (AIE) properties.[8]These materials exhibit opposite properties of the more commonly observed aggregation caused quenching (ACQ)

and, in fact, have excellent fluorescence quantum efficiencies in the solid-state compared to near quenching in solution. The original material that was found to exhibit such intriguing optical properties was 1-methyl-1, 2, 3, 4, 5-pentaphenylsilole and was first discovered by B. Z. Tang's group.[9] Within this last year other materials based on cyanostilbenes,[10] fumaronitrile,[11] dibenzosuberenylidene,[12] carborane,[13] 9,10-distyrylanthracene,[14] phenylpyrrole,[15] spiropyran,[16] and even some organometallic iridium materials[17] have also demonstrated AIE activity. However, besides silole-based materials, probably the more active player within the AIE research field has been tetraphenylethene (TPE) and its derivatives.[18] TPE-based materials are easy in synthesis and modify, exhibit high AIE-effect values (extent of emission enhancement), and display excellent solid-state fluorescence quantum yields (near quantitative).[8,18] Due to these aspects TPE-based materials have paid increased attention in the fields of OLEDs and chemo/biosensors with recent review articles being published regarding both topics.[19] We also designed and synthesized two TPE-phenanthroline conjugates, which exhibit different fluorescence behavior to metal ions in aggregate state and in free molecule state.[20]

Due to the excellent hole-transporting properties of carbazole and the high photoluminescence quantum yields of TPE it has been the subject of several research papers to combine these two units together. This has also been successfully achieved using fluorene as its major core component, in which hindered internal bond motions of the TPE end-cap groups were responsible for the enhanced fluorescence in the "aggregate" state. The connection between TPE and carbazole consist of 9-*N*-position, 3,6-position linkage, both at 9-*N*-position and 3,6-position and in conjugated hyperbranched polymers.[21] What's more, variety of highly emissive solid emitters with high T_g[22] and good hole transporting properties[23] have been synthesized and applied to OLED or PLED. From our recent success regarding the synthesis of 1, 3, 6- and 1, 3, 6, 8- brominated carbazole materials and the lack of investigations at the 2, 7-positions we believe it was important to complete this research topic. Therefore, in attempt to tie together our previous research works we have fully incorporated TPE into carbazole at all the possible connection sites (1, 2, 3, 6, 7, and 8-positions, see **Figure 1**) and investigate their comparative thermal, optical, electroluminescence and AIE properties. Due to the susceptibility of TPE to undergo photo-oxidation,[24] the photo-oxidative stability was fully evaluated in solution and solid-state, in which the latter is especially important for OLED applications.

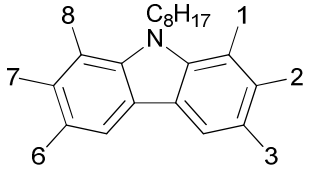

Figure 1 1, 2, 3, 6, 7 and 8 positions located on the carbazole ring.

Herein, we report the synthesis of tetraphenylethene-decorated carbazoles at all the possible connection sites (1 and 8, 3 and 6, 2 and 7-positions) via the selective bromination of carbazole followed by Suzuki cross-coupling reaction. The thermal, optical, photochemical, electrochemical and electroluminescence properties of tetraphenylethene-decorated carbazoles have been studied comparatively.

Experimental

All commercially available starting materials, reagents and solvents were used as supplied, unless otherwise stated, and were purchased from Aladdin, Acros Organics and Puyang Huicheng Chemical Co. Ltd. All reactions were carried out under a dry nitrogen atmosphere unless water was used as a solvent or reagent and the temperatures were measured externally. For brominations no nitrogen was used to prevent contamination of the nitrogen line. Tetrahydrofuran (THF) and toluene were dried using sodium wire and benzophenone as indicator. Dichloromethane (DCM) was dried over calcium sulfate and distilled. Reported yields are isolated yields. Purification of most intermediates and all final products was accomplished in most cases by gravity column chromatography, using silica gel. For qualitative purity tests of all intermediates and final products, a single spot (visualized using UV-light at 254 nm and 365 nm) was obtained. Elemental analysis was used for quantitative purity checks of all final products. ^{1}H NMR spectra are reported in parts per million (ppm) relative to tetramethylsilane as an internal standard.

The synthesis procedure of different bromo substitute carbazoles and TPE boronic acid could be found in previous work.[6]

1: Cz-1TPE: Into a 50 mL two-neck flask, 3-bromo-9-octyl-carbazole (0.20 g, 0.56 mmol), TPE-boronic acid (0.23 g, 0.61 mmol), K_2CO_3 (0.46 g, 3.36 mmol), PTC ($(C_4H_9)_4NHSO_4$) (0.01 g, 0.056 mmol) and $Pd(PPh_3)_4$ (0.05 g, 0.056 mmol) were added. Under N_2 atmosphere, 10 mL toluene and 5 mL H_2O were added in. The reactant was heated to 90℃ and stirred for 1 day. After the reaction finished, the organic layer was washed with water (10 mL×3), extracted by toluene, and then combined. The organic was dried by $MgSO_4$, filtrated and prepared for column chromatography on silica gel with 20% DCM-80% petroleum ether (PE) as eluent after evaporating the solvent. 0.28 g light yellow-green solid was obtained, yield 82%. ^{1}H NMR (600 MHz, $CDCl_3$): δ8.27 (s, 1H), 8.11 (d, 1H, J = 7.62 Hz), 7.67 (d, 1H, J = 7.26 Hz), 7.47 (m, 3H), 7.40 (m, 2H), 7.22 (d, 1H, J = 7.26 Hz), 7.00-7.20 (m, 17H), 4.30 (t, 2H, J = 7.20Hz), 1.89 (m, 2H), 1.10-1.40 (m, 10H), 0.80 (t, 3H, J = 6.60Hz); ^{13}C NMR ($CDCl_3$): δ143.92, 141.80, 140.89, 140.86, 140.78, 139.95, 139.89, 131.84, 131.69, 131.51, 131.43, 127.81, 127.70, 127.66, 126.46, 126.38, 126.27, 125.75, 124.94, 123.31, 123.02, 120.42, 118.87, 118.63, 108.84, 43.22, 31.82, 29.41, 29.20, 29.03, 27.35, 22.64, 14.10; MS (APCI) calcd. for $C_{46}H_{33}N$: 609.84; Found: $[M^+]$+H 610.5; Anal. calc. for $C_{46}H_{33}N$: C90.60, H7.11, N2.30; Found: C 90.45, H 6.92, N 2.44.

2: Cz-2TPE (3, 6): Compound **2** was synthesized similarly as described for the synthesis of **1**. Yellow green solid, 88% yield (380 mg).^{1}H NMR (600 MHz, $CDCl_3$): δ = 8.27 (s, 2H), 7.67 (d, 2H, J = 8.46 Hz), 7.47(m, 4H), 7.40 (d, 2H, J = 8.46 Hz), 7.05-7.15 (m, 34H), 4.29 (t, 2H, J = 7.08 Hz), 1.88 (m, 2H), 1.20-1.30 (m, 10H), 0.88 (t, 3H, J = 6.72 Hz); ^{13}C NMR ($CDCl_3$): δ143.96, 143.91, 141.86, 140.89, 140.77, 140.36, 139.80, 131.85, 131.52, 131.43, 127.81, 127.7, 127.66, 126.47, 126.39, 126.26, 125.06, 123.50, 118.71, 108.99, 43.33, 31.97, 31.82, 29.74, 29.70, 29.41, 29.21, 29.06, 27.34, 22.74, 22.64, 14.17, 14.11; MS (APCI) calcd. For $C_{72}H_{61}N$ 940.26; Found: [M+H] 940.8; Anal. calc. for $C_{72}H_{61}N$: C91.97, H6.54, N1.49; Found: C92.40, H6.64, N1.33.

3: Cz-3TPE: Compound **3** was synthesized similarly as described for the synthesis of **1**. Yellow green solid, 74% yield (360 mg). ^{1}H NMR (600 MHz, $CDCl_3$): δ 8.29 (dd, 2H, J = 15.3 Hz), 7.66 (dd, 1H, J = 8.52 Hz), 7.47 (d, 4H, J = 7.02 Hz), 7.41 (d, 1H, J = 1.62 Hz), 7.37 (d, 1H, J = 8.52 Hz), 7.23 (s, 2H), 7.00-7.24 (m, 51H), 3.84 (t, 2H, 7.08Hz), 1.10-1.40 (m, 10H), 0.88 (t, 3H, J = 7.14Hz); ^{13}C NMR ($CDCl_3$): δ143.93, 143.89, 143.85, 143.80, 143.73, 143.69, 142.89, 141.37, 140.87, 140.74, 140.56, 139.29, 138.40, 131.50, 131.41, 131.34, 131.04, 129.10, 128.53, 127.83, 127.79, 127.68, 127.65, 126.68, 126.58, 126.53, 126.45, 126.37, 126.23, 125.10, 123.80, 118.41, 117.47, 31.77, 29.72, 29.68, 29.39, 29.30, 29.02, 28.89, 26.60, 22.72, 22.63, 14.12; MS (APCI) calcd. for $C_{98}H_{79}N$: 1270.68; found: [M+] 1271.0; Anal. calc. for $C_{98}H_{79}N$: C92.63, H6.27, N1.10; Found C92.85, H6.29, N1.05.

4: Cz-4TPE: Compound **4** was synthesized similarly as described for the synthesis of **1**. Yellow green solid, 44% yield (240 mg). ^{1}H NMR (600 MHz, $CDCl_3$): δ8.23 (s, 2H), 7.48 (m, 6H), 7.27 (d, 4H, J = 7.98 Hz), 7.00-7.20 (m, 68H), 3.40 (t, 2H), 0.90-1.30 (m, 12H), 0.80 (t, 3H, J = 7.26Hz); ^{13}C NMR ($CDCl_3$): δ143.87, 143.82, 143.74, 142.66, 141.37, 140.57, 131.50, 131.47, 131.42, 131.36, 127.83, 127.81, 127.73, 127.68, 127.66, 126.69, 126.63, 126.54, 126.47, 126.40, 117.24, 31.67, 28.94, 28.85, 25.89, 22.85, 22.69, 22.62, 14.13; MS (APCI) calcd. for $C_{124}H_{97}N$: 1601.10; Found: [M+]1601.1; Anal. calc. for $C_{124}H_{97}N$: C93.02, H6.11, N 0.87; Found: C93.04, H6.19, N0.82.

5: Cz-2TPE (2, 7): Compound **5** was synthesized similarly as described for the synthesis of **1**. Yellow green solid, 81% yield (350 mg). ^{1}H NMR (600 MHz, $CDCl_3$): δ 8.07 (d, 2H, J = 8.04 Hz), 7.52 (s, 2H), 7.49 (d, 4H, J = 8.22 Hz), 7.43 (dd, 2H, J = 8.16 Hz), 7.00-7.20 (m, 34H), 4.32 (t, 2H, J = 7.14 Hz), 1.89 (m, 2H), 1.10-1.45 (m, 10H), 0.85 (t, 3H, J = 6.60 Hz); ^{13}C NMR ($CDCl_3$): δ143.87, 143.84, 142.58, 141.55, 141.09, 140.64, 139.89, 138.53, 131.85, 131.49, 131.43, 131.42, 127.84, 127.74, 127.68, 126.65, 126.52, 126.45, 121.90, 120.53, 118.50, 106.86, 43.05, 31.84, 29.42, 29.22, 29.05, 27.34, 22.65, 14.13. MS (APCI) calcd. for $C_{72}H_{61}N$: 940.26; Found: [M+]+H 940.9; Anal. calc. for $C_{72}H_{61}N$: C91.97, H6.54, N1.49; Found: C92.25, H6.45, N, 1.52.

Results and discussion

Synthesis

Carbazole-based materials used in organic semiconductor research are usually designed and subsequently built from the accessible points at the *N*-9-position, 3, 6-positions and the 2, 7 positions. The functionalisation of the 9-*N*-position and 3, 6-positions are relatively straightforward and requires Ullmann condensations/nucleophilic substitutions and bromination, respectively. Due to the fact that electrophilic substitution of carbazole occurs at the activated 3, 6-positions, the 2, 7-dibromo carbazole requires an alternative synthetic pathway. One alternative pathway involves the nitration of 4, 4'-dibromo-1-1'-biphenyl to yield its mono-nitro derivative, which can be subsequently ring-closed using PPh_3 in 1,2-dichlorobenzene (*o*-DCB) to yield 2, 7-dibromo-9*H*-carbazole. 3-Bromocarbazole and 3, 6-dibromocarbazole are easily prepared using N-Bromosuccinimide (NBS) in N, N-Dimethylformamide (DMF) at room temperature. The synthesis of 1, 3, 6-tribromocarbazole has recently been reported by our group and can prepared by treating 9-octylcarbazole with NBS-silica gel in $CHCl_3$ in excellent yield and purity. 1, 3, 6, 8-Tetrabromocarbazole can also be synthesised at room temperature using $Br_2/FeCl_3$ in CH_2Cl_2. The *N*-position was functionalised with octyl chains by *N*-alkylation using NaOH, a two-phase toluene-water solvent system and 1-bromooctane. Standard Pd-catalysed Suzuki couplings were performed to prepare the final materials, Cz-1TPE, Cz-2 TPE(3,6), Cz-2TPE(2,7), Cz-3TPE and Cz-4TPE (**Scheme 1**).

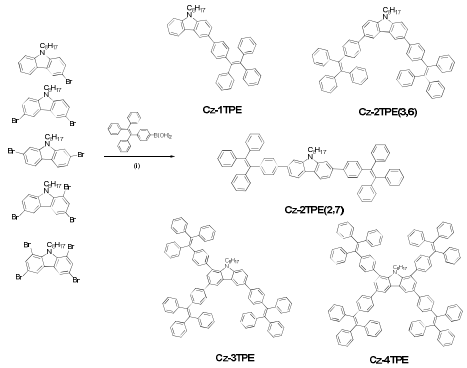

Scheme 1 Synthesis of the Carbazole-TPE materials.

Thermal Properties

Thermal properties of Cz (1-4) TPE are shown in **Table 1**.

Table 1 Photo-physical and thermal parameters of Cz-TPEs.

	λ_{abs}(nm) Soln[a]	λ_{em}(nm) Film	Φ_F (%) Soln[b]	Φ_F (%) Film[c]	T_g/T_d[d] [℃]	D[e] (nm)
Cz-1TPE	290/334	483	0.37	44.6	20.7/331	125.4
Cz-2TPE	299/337	487	0.16	50.5	65.4/449	127.5
Cz-3TPE	318	488	0.23	61.1	70/493	136.6
Cz-4TPE	326	485	0.18	57.6	94.3/463	144.1
Cz-2TPE(2,7)	360	483	0.22	47.5	137.5/443	115

[a] Soln = solution (10 μM in THF), λ_{abs} = absorption maximum, λ_{em} = PL maximum with excitation at 340 nm; [b] Fluorescence quantum yield measured in THF using 9, 10-diphenylanthracene (Φ_F = 90% in cyclohexane) as standard, [c] The samples were fabricated by spin-coating with Cz-TPEs dissolved in PMMA solution (5 g PMMA in 50 ml distilled DCM), 1 mg of Cz-TPEs in 1 ml of PMMA solution; [d] T_d is from TGA spectra with 5% weight loss of the sample; [e] the diameters of nanoparticles for AIE are measured dynamic light scattering.

The glass transition temperatures (T_g) were evaluated by differential scanning calorimetry (DSC) and differential thermal analysis (DTA). From **Figure 2B**, all these new synthesized Cz-TPEs exhibited relative high thermal stabilities with T_d (corresponding to 5% weight loss) ranging from 331, 449, 493, 463 to 443 °C for Cz-1TPE, Cz-2TPE, Cz-3TPE, Cz-4TPE, Cz-2TPE (2, 7), respectively. As expected the DSC scans (see **Figure 2A**) of all 5 fluorophores show a first order transition temperature above room temperature, which represents a glass transition temperature (T_g). Only a crystallization exotherm was observed for Cz-2TPE (2, 7) and for the other carbazole-TPE materials no crystallization exotherms are observed during the cooling and heating cycles. Cz (1-4) TPE were isolated as amorphous materials due to the absence of an endothermic melting peak on the first heating cycle. This is probably due to the high viscosity of the amorphous state. The highest T_g value was observed for Cz-4TPE (138 °C), which has the highest molecular weight and perhaps the most hindered free volume. We have also confirmed the amorphous nature of these materials by XRD analysis (see **Figure 2C**), in which the diffraction curve shows the characteristic amorphous halo without sharp crystalline diffractions.

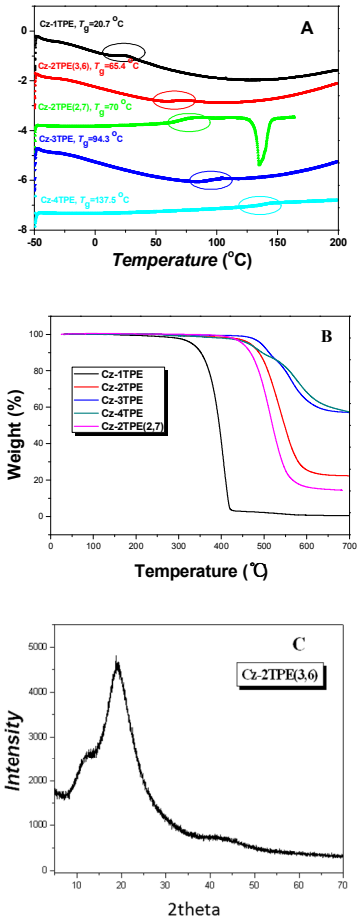

Figure 2 (A) DSC and **(B)** TGA thermograms of Cz-1TPE, Cz-2TPE (3, 6), Cz-2TPE (2, 7), Cz-3TPE and Cz-4TPE recorded under N_2 at a heating rate of 15 and 10 ℃/min, **(C)** XRD pattern of the as-synthesised Cz-2TPE (3, 6) after 6 months of the initial isolation is featureless. The lack of diffraction peaks indicates that Cz-2TPE (3, 6) remains as an amorphous material for a long period of time without crystallisation.

Photo-physical and Aggregation Induced Emission (AIE)

Static state UV-vis absorption. The absorption spectra of Cz-TPEs in THF (10^{-5} M) are shown in Figure 3. In the same concentration of 10^{-5} M, the absorbance (molar extinction coeffient ε) at the maximum wavelength is in the following order: Cz-1TPE＜Cz-2TPE≈Cz-3TPE＜Cz-4TPE. Two peaks at 290 nm and 334 nm are observed for Cz-1TPE, which is 35nm red shifted compared to TPE (299 nm) molecules alone. The absorption spectrum of Cz-2TPE is more red-shifted to that of Cz-1TPE with two peaks at 299 nm and 337 nm, which might be because two TPEs at both 3 and 6 position of carbazole form a larger conjugation than that of Cz-1TPE. The absorption spectra of Cz-3TPE and Cz-4TPE are very broad between 270 nm and 360 nm with peak at 318 nm and 326 nm respectively.

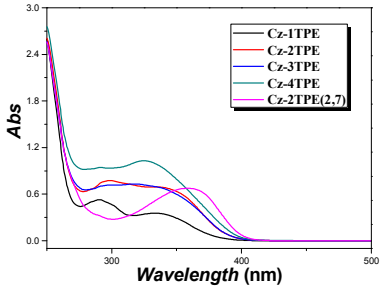

Figure 3 UV-vis absorption spectra of Cz-TPEs in THF with concentration equal to 10-5M.

Overall the Cz-TPEs (TPE at 1, 3, 6, 8 positions), the absorption spectra are similar, while Cz-2TPE (2, 7) is quite different. Only one defined peak at 360 nm is observed for Cz-2TPE (2, 7), which is 23 nm red-shifted compared with Cz-2TPE (3, 6). This could be explained by former mechanism proposed by Bea M. W. Langeveld.[1d] We can see from **Figure 4** that the conjugation length of Cz-TPEs at 1, 3, 6, 8 positions are isolated in one phenyl ring of carbazole and TPE, while at 2 and 7 position form a whole a conjugation of the molecule. Since more TPEs connected to 1 and/or 8 position do not enlarge the conjugation of the molecule, they exhibit very little difference in absorption spectra.

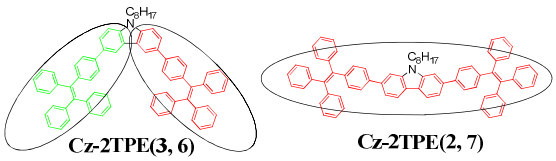

Figure 4 Molecule structure of Cz-2TPE (3, 6) and Cz-2TPE (2, 7) and the oval represent the conjugation of the molecule

Aggregation induced emission. The AIE behavior is investigated by monitoring the change in PL intensity with the addition of increasing amounts of water in a THF/water solvent mixture. Here, THF acts as the solvent and water acts as the non-solvent. Typical AIE behavior is observed by a transition from isolated molecules to nano-aggregates at a critical concentration of water. This results in a corresponding increase in the PL intensity. The experiment is carried on by adding 20 μL Cz-TPEs solution (10^{-3} M in THF) using a microsyringe (25 μL) to a 2.0 ml mixture of THF-water (f_w= 0-90%). In this way, the

concentration is ascertained to be 10^{-5} M in different f_w. During the experiment, all the aggregates were homogeneous with no precipitates.

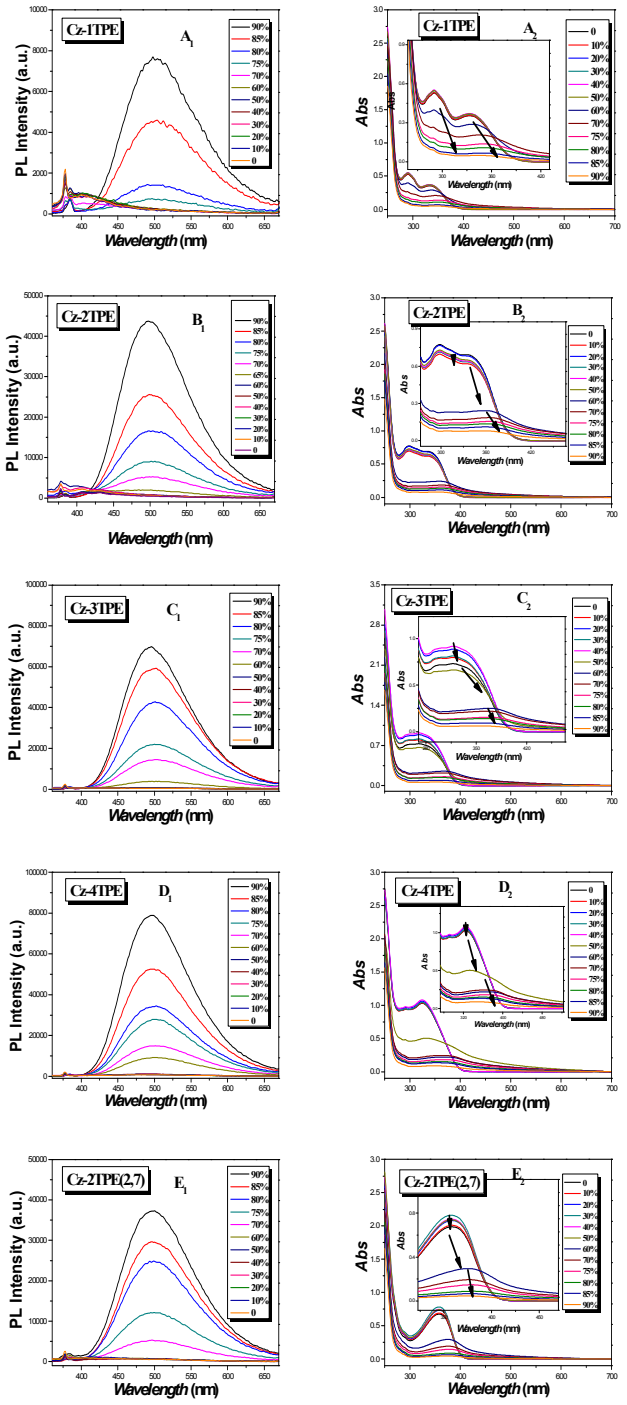

Figure 5 PL spectra and UV-vis spectra of (**A_1, A_2**) Cz-1TPE, (**B_1, B_2**) Cz-2TPE, (**C_1, C_2**) Cz-3TPE, (**D_1, D_2**) Cz-4TPE and (**E_1, E_2**) Cz-2TPE (2, 7) in water-THF mixture with f_w changing from 0 to 90%.

In THF, all the Cz-TPEs are non-fluorescent. Cz-1TPE is non-fluorescent in f_w = 0-75%, and then an abroad peak around 500nm at f_w = 80% is observed. The PL intensity increases sharply with f_w = 90% for 37.5 times compared to f_w = 0% (see **Figure 5A$_1$**). The corresponding UV-vis absorption in f_w = 0-50% nearly unchanged. When the f_w gradually increases to 90%, the two peaks at 290 nm and 344 nm slowly red-shifted with decreases in intensity and a long tail around 400-600 nm is observed, simultaneously (see **Figure 5A$_2$**). The decreases in absorption and long tail around 400-600 nm is because of nano-aggregates form in high f_w. This has been proved by differential light scattering (DLS) data (see **Table 1** and **Figure S3**). The diameter of nano-aggregate in f_w = 90% of Cz-1TPE is calculated to be 125.4 nm. The other Cz-TPEs are similar to that of Cz-1TPE and the diameters of nano-aggregate in f_w = 90% for Cz-2TPE, Cz-3TPE, Cz-4TPE, Cz-2TPE (2, 7) are calculated to be 127.5, 136.6, 144.1 and 115 nm.

It is interesting to note that the f_w that the emission begins to "light up" is in the following order: Cz-4TPE (f_w = 60%) ≈ Cz-3TPE (f_w = 60%) < Cz-2TPE (3, 6) (f_w = 65%) <Cz-2TPE (2, 7) (f_w = 60%) < Cz-1TPE (f_w = 75%). This phenomenon could also be witnessed from the photos in **Figure 6**. With more TPE attached to the carbazole core, the fluorescence becomes more "earlier" to light up. This might be because more TPEs connecting to the carbazole increase the molecular weight decrease the solubility in organic solvent and become much easier to form nano-aggregates as a result.

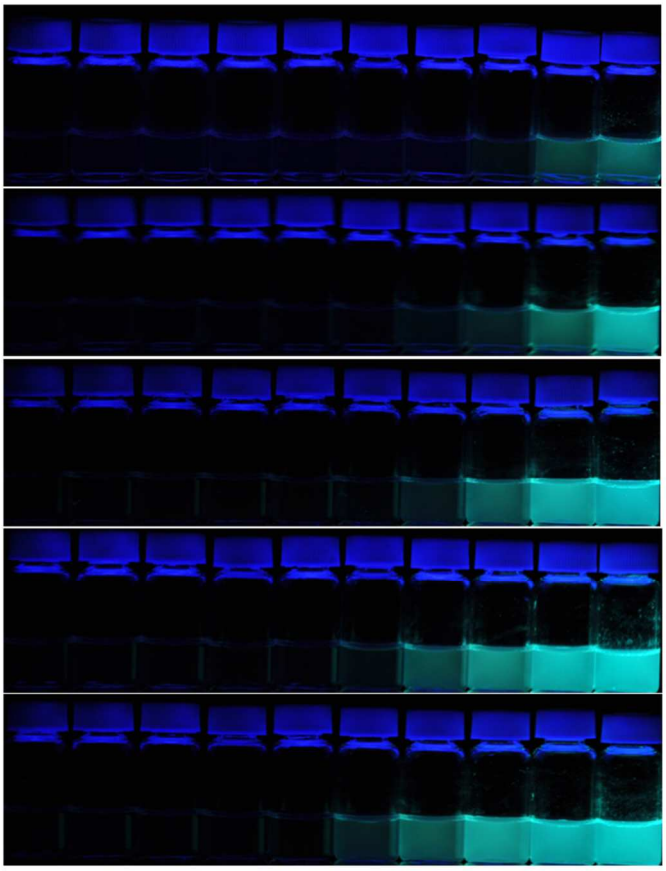

Figure 6 From left side to right side with f_w changing from 0% to 90%; from upside to downside is Cz-1TPE, Cz-2TPE(3,6), Cz-2TPE(2,7), Cz-3TPE, Cz-4TPE concentration 10^{-5}mol/L; the photos are taken under UV light of 365nm illumination.

The plot of (I/I_0-1) -f_w is made to compare the AIE properties of the Cz-TPEs. We can see from **Figure 7** that Cz-1TPE＜Cz-2TPE (2, 7) ≈Cz-2TPE (3, 6)＜Cz-4TPE＜Cz-3TPE. Except Cz-4TPE is weaker than that of Cz-3TPE, we can conclude that when more TPEs are connected to the carbazole, the AIE properties have been strengthen. To investigate the AIE more quantitatively, quantum yield for all the Cz-TPEs in PMMA film and pure THF solution is studied, using DPA as standard materials (see **Figure S1**). The fluorescent quantum yields are 44.6%, 50.5%, 61.1%, 57.6% and 47.5% in PMMA film compared to 0.37%, 0.16%, 0.23%, 0.18% and 0.22% in THF solution for Cz-1TPE, Cz-2TPE, Cz-3TPE, Cz-4TPE and Cz-2TPE (2, 7), respectively (see **Table 1**). The fluorescent quantum yields of Cz-TPEs in PMMA film are consistent with the (I/I_0-1) -f_w.

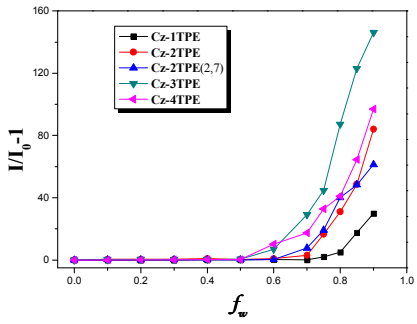

Figure 7 Plots of (I/I_0-1) values as a function of f_w in THF/water mixtures of Cz-TPEs, in which I_0 is the PL maximum intensity in pure THF solution.

Photo-Oxidation

Photo oxidation in dilute solution. The experiments are performed by dissolving Cz-TPEs in distilled THF (concentration equal 10^{-5} mol/L) and exposing under UV light (302 nm, 0.85 mW/cm^2) with different time. Cz-TPEs are no fluorescent in THF because of their AIE nature. After UV light irradiation for 5 min, Cz-1TPE exhibits two peaks at 391 nm and 404 nm. The fluorescent intensity enhances sharply with further increasing the irradiation time. And the UV-Vis absorption spectra peak at 335 nm and 293 nm blue shift gradually to 327 nm and 290 nm with an isosbestic point at 312 nm (Figure 8A_2). The fluorescent intensity of Cz-2TPE solution slightly increased in the first 30 min. After 45 min irradiation, it increases 5.7 times with 3 defined peaks at 407 nm, 430 nm and 456 nm. By extending irradiation time, it increases by 21.1 times and the peaks at 430 nm and 456 nm become mistiness with one strong peak at 406 nm.

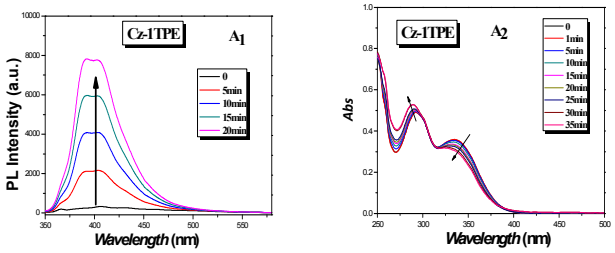

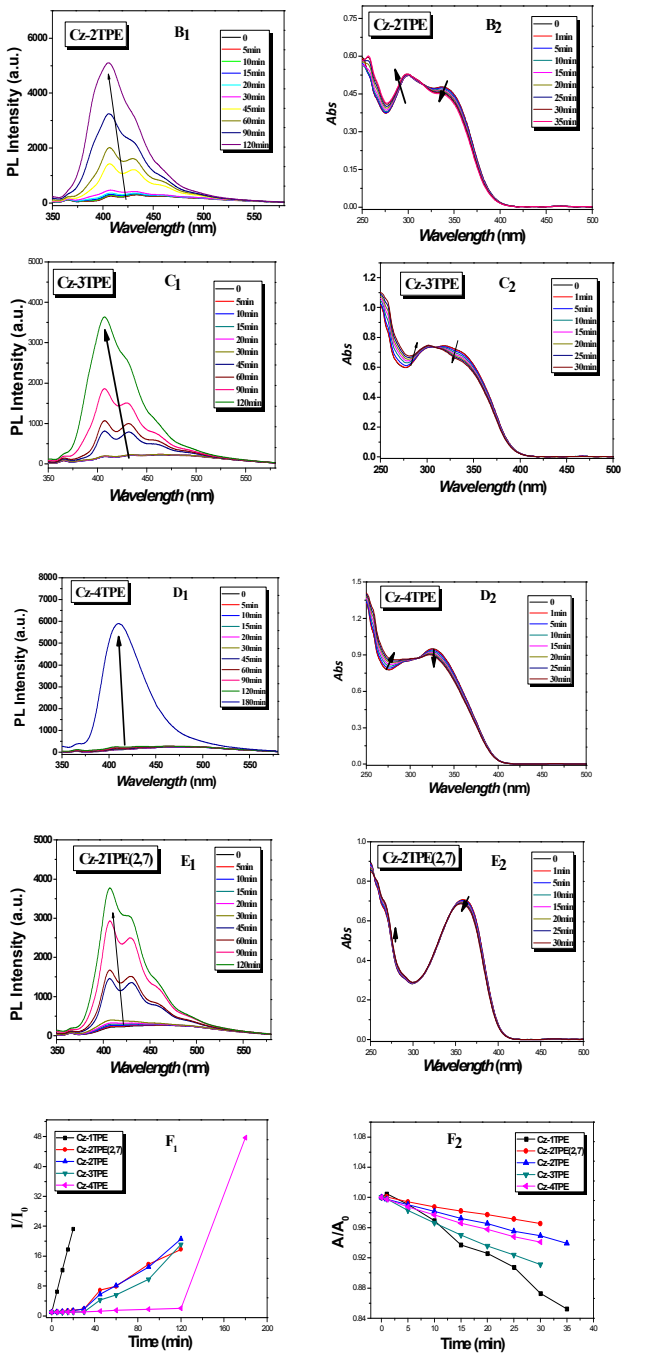

Figure 8 PL spectra and corresponding UV-Vis spectra of (**A_1, A_2**) Cz-1TPE, (**B_1, B_2**) Cz-2TPE, (**C_1, C_2**) Cz-3TPE, (**D_1, D_2**) Cz-4TPE and (**E_1, E_2**) Cz-2TPE (2, 7) in distilled THF of concentration equal to 10^{-5}M with different UV (302 nm, 0.85 mW/cm^2) irradiation time; (**F_1**) plot of **I/I_0** (the fluorescence intensity at 407nm) with different UV(302nm) irradiation time; (**F_2**) plot of **A/A_0** (the Abs at 335nm for Cz-1TPE, 338nm for Cz-2TPE, 338nm for Cz-3TPE, 326nm for Cz-4TPE, 360nm for Cz-2TPE (2,7)) with different UV (302nm) irradiation time.

The corresponding UV-Vis absorption peaks at 338 nm and 301 nm blue shift gradually to 334 nm and 298 nm with an isosbestic point at 316 nm. (Figure 8B_2) Similar to Cz-2TPE, the fluorescent intensity of Cz-3TPE and Cz-2TPE (2, 7)

solution nearly unchanged in the first 30 min and three defined peaks are observed in 45 min which are 407 nm, 432 nm and 456 nm. These peaks are identical to that of Cz-2TPE after UV irradiation, which indicates a similar process in the photo-oxidation process. The absorption peak of Cz-3TPE at 323 nm decreases and the peak at 301 nm increases with an isosbestic point at 310 nm. (Figure 8C_2) The absorption peak of Cz-2TPE (2, 7) at 360 nm decreases and an isosbestic point at 344 nm was observed after UV irradiation. (Figure 8E_2) The fluorescent spectra of Cz-4TPE nearly unchanged even irradiated for 2 h. However, the absorption spectra of Cz-4TPE clearly changes: the peak at 326 nm decreases and absorbance increase around 250-300 nm with an isosbestic point at 310 nm. (Figure 8D_2) After further irradiated it for 1 h, a strong peak at 410 nm appears. This indicates that there exists an induced period of fluorescence occurrence for TPE multi-substituted carbazole. The oxidation reaction of TPE continued upon UV irradiation, though. Only when the all-oxidation of four TPEs was finished, the fluorescence increases abruptly.

HPLC analysis. HPLC analysis is performed to detect the photo-oxidation process. In this case, we choose the simplest molecule Cz-1TPE as an example. We investigate the effect of different concentration of the samples, which are 10^{-3} M, 10^{-4} M, 10^{-5} M, and different irradiation time: 1 h, 2 h and 3 h to the photo-oxidation process. Cz-1TPE is first dissolved in THF with concentration divided into three groups: 10^{-3}, 10^{-4} and 10^{-5} mol L^{-1}. Then each group is irradiated under UV lamp (302 nm) for 1 h, 2 h and 3 h. These samples are put in open air to evaporate the solvent THF and then they are used for HPLC directly using hexane as eluent.

Before we did the experiments, we first measured the HPLC spectrum of Cz-1TPE using hexane as eluent (the retention time is 18.4 min for Cz-1TPE without UV irradiation). Thus the peak at 18.4 min can be attributed to Cz-1TPE and the two peaks at 27.8 min and 29.4 min are the photo-oxidation products. We normalize the intensity of the peak 18.4 min and compare the peak intensity at 27.8 min and 29.4 min (see Figure 9A) for every sample. In sample with [conc] = 10^{-3} M, after 1 h irradiation, the integral area at 27.8 min and 29.4 min are 0.50% and 0.89%. With longer irradiation time of 2 h and 3 h, they increase to 0.98% (27.8 min), 1.86% (29.4 min) and 1.42% (27.8 min), 2.52% (29.4 min). These changes are very tiny but identical to indicate the changes after UV irradiation. When the sample is 10 times and 100 times dilute to 10^{-4} M and 10^{-5} M, the intensity exhibits higher changes at 27.8 min and 29.4 min, which indicates more Cz-1TPE convert to photo-oxidation products. The detail changes of peak 1 (27.8 min) and peak 2 (29.4 min) could be seen from Figure 9B and 9C with different UV irradiation time and concentration. It is clear that with longer irradiation time and more dilute concentration, the conversion of photo-oxidation improves from the HPLC results.

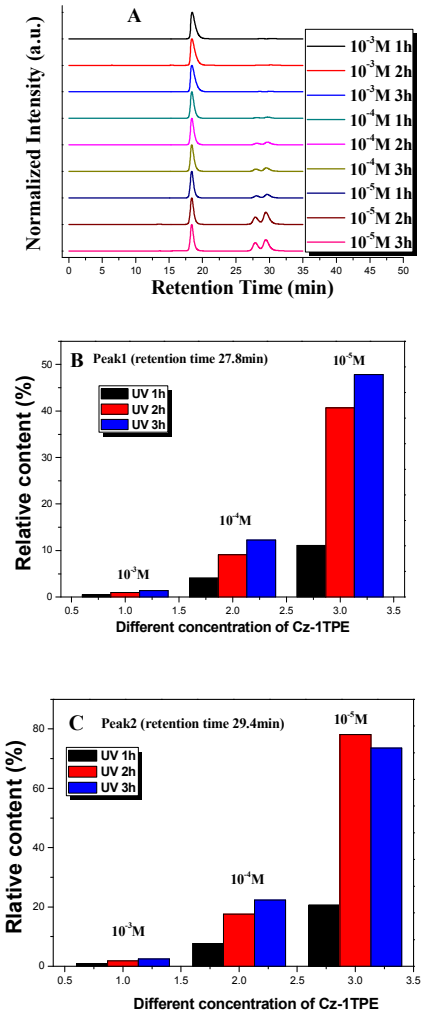

Figure 9 (**A**) HPLC chromatogram of Cz-1TPE with different UV irradiation time (1 h, 2 h, 3 h) and different concentration (10^{-3}, 10^{-4} and 10^{-5} mol L^{-1}). HPLC analysis was performed using an analytical column equipped with a UV detector; the mobile phase was hexane with a flow rate of 1.0 mL/min (range; 0.005, inject volume; 20 µL,detection wavelength; 312 nm), Insert: expanded image of 10^{-3} M around retention time between 27 min to 33 min; (**B**) Plot of relative content of peak 1 (retention time 27.8 min) with different concentration (10^{-3} M, 10^{-4} M, 10^{-5} M) and UV irradiation time (1 h. 2 h, 3 h); (**C**) Plot of relative content of peak 2 (retention time 29.4 min) with different concentration (10^{-3} M, 10^{-4} M, 10^{-5} M) and UV irradiation time (1 h. 2 h, 3 h).

^{1}H NMR and LC-MS analysis. We further investigate the photo-oxidation of Cz-1TPE in solution by ^{1}H NMR and LC-MS. The experiment was performed by exposing the NMR tube with samples under UV light for 3 h. The corresponding ^{1}H NMR spectra of Cz-1TPE before (**A**) and after (**B**) UV (302 nm, 3 h) light irradiation are presented in **Figure S17**. Basically, the chemical shift of Cz-1TPE before and after UV irradiation nearly unchanged (see ESI Figure S15) except a few multi peaks around δ4.3 (***N-CH$_2$***) was observed. As we set the integral area around δ4.3 as 2, the integral area around δ7.0-7.22, which belongs to the **TPE** group (17 Ar-H, in red) decreases from 16.85 to 16.14. It can be explained that the

decrease of relative integral area around δ7.0-7.22 is attributed to the photocyclisation of phenyl rings in TPE.

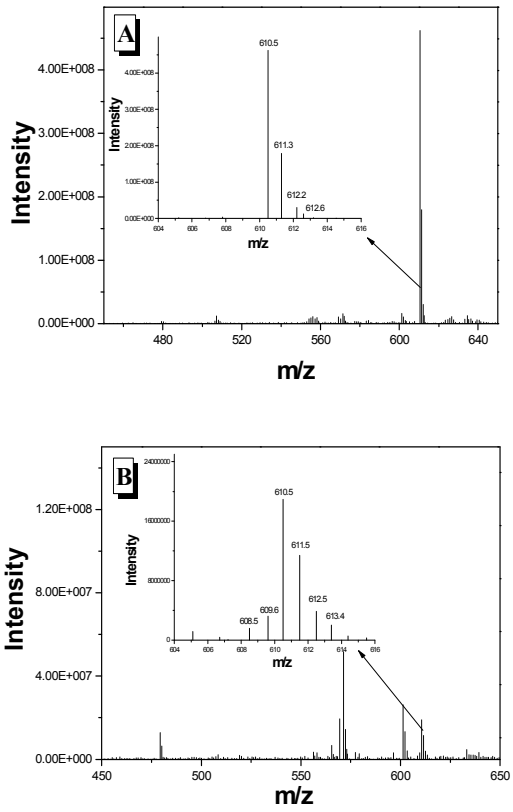

Figure 10 LC-MS spectra of Cz-1TPE (A) before and (B) after UV light (302 nm, 3 h) irradiation.

After the ^{1}H NMR experiments we use the photo-oxidized products directly to LC-MS measurement. The LC-MS spectra of Cz-1TPE before and after UV (302 nm, 3 h) are presented in **Figure 10**. We can see clearly the 610.5 (M+1) signal of Cz-1TPE (Mw= 609.8) and corresponding isotope signals 611.3 and 612.2 from Figure 12 (**A**). After UV irradiation two new signals of 608.5 and 609.6 appear together with the three peaks from the Cz-1TPE (610.5, 611.5 and 612.5), which are exactly 2 H loss from Cz-1TPE. These results directly support our photo-oxidation mechanism. Meanwhile, it is worth to emphasize that the photo-oxidation was not 100% converted to the photo-oxidation products, which could be witnessed from both the ^{1}H NMR and LC-MS measurements. This is because the concentration of the sample for ^{1}H NMR usually needs to be high (much higher than 10^{-5} mol/L). In our case, 5.5 mg Cz-1TPE was dissolved in 0.6 ml $CDCl_3$ and the concentration is calculated to be 1.5×10^{-2} mol/L. According to the former HPLC analysis when the concentration increases, the photo-oxidation conversion will decrease dramatically. And the similarity of the photo-oxidation products and Cz-1TPE makes it more difficult to discriminate the changes from the ^{1}H NMR analysis. As we know, usually photo chemical reactions are much more complex than normal chemical reactions, and if the UV irradiation time is too long, other unpredictable changes might happen.

Photo Oxidation in Pure thin film. In order to investigate the photo-oxidation of Cz-TPEs practically, we apply the experiment in pure thin films, since an important application of TPE molecules are in OLEDs. The samples are prepared by dissolving Cz-TPEs in distilled THF. Then the solution is dropped on to glasses. By spin-coating method (400 rad/s, 1 min), pure thin film (thickness: ~40 nm) of Cz-TPE samples are made. The thickness of the prepared film is calculated and presented in ESI Figure S3.

Cz-1TPE emits strongly in thin film at 483 nm. The λ_{em} of Cz-2TPE, Cz-3TPE, Cz-4TPE and Cz-2TPE (2, 7) are 487 nm, 486 nm, 483 nm and 489 nm, respectively (**Figure 11**). The fluorescent intensity gradually decreased in the first 30min. After 90 min irradiation, the fluorescence of Cz-1TPE quenches to 1% of the original intensity and blue shift to 460 nm. Similar phenomenon is observed for other Cz-TPEs. The fluorescent intensity decreases to 2%, 1.6%, 0.7% and 1.4% for Cz-2TPE, Cz-3TPE, Cz-4TPE and Cz-2TPE (2, 7), respectively. The plot of I/I_0 (fluorescence intensity at 483 nm) with UV different irradiation time is shown in **Figure 11F**.

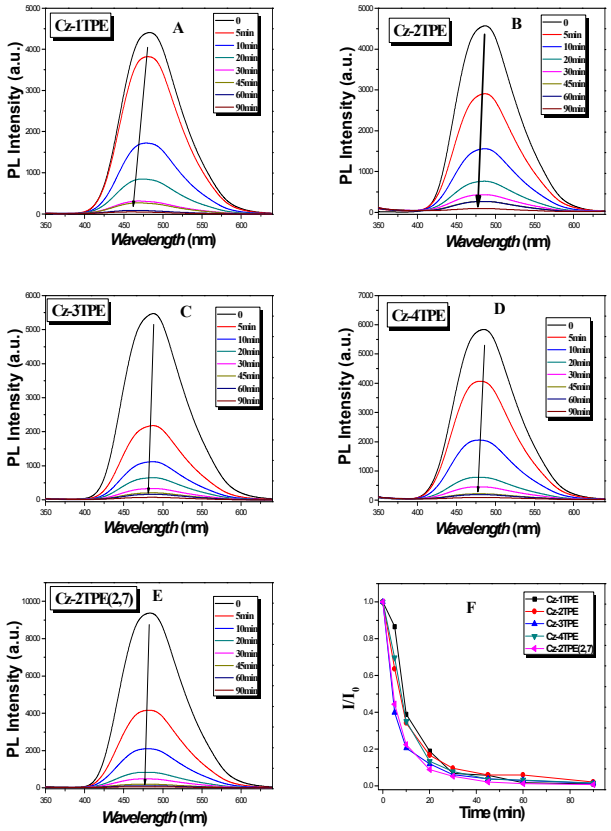

Figure 11 PL spectra of Cz-TPEs (A) Cz-1TPE, (B) Cz-2TPE, (C) Cz-3TPE, (D) Cz-4TPE, (E) Cz-2TPE (2, 7) in pure thin film with different irradiation time: 0, 5 min, 10 min,20 min, 30 min, 45 min, 60 min and 90 min and (F) plot of I/I0 (fluorescence intensity at 483 nm) with different irradiation time.

From the photo-oxidation experiment we can conclude the following characters of photo-oxidation: 1) in THF solutions, the non-fluorescent Cz-TPEs solutions emit strong blue light around 410 nm after proper time of UV irradiation; 2) The absorbance peaks of Cz-TPEs decreases and blue-shifted with a remarkable isosbetic point around 310 nm (Cz-2TPE (2, 7) is an exception because of its better conjugation (λ_{max}=360 nm), also an isosbestic point at 344 nm was observed); 3) in thin film, the fluorescence quenches and blue shifts to shorter wavelength after proper time of UV irradiation. These characters strongly indicate their similarity in photo-oxidation process, which could also be induced from the similar structures (**Figure 12A and 12B**). According to the former investigation in photo-oxidation of TPE molecules,[24] we proposed the following process to explain the photo-oxidation here. Under long time UV irradiation, the TPE molecule could be oxidized to form a diphenylphenanthrene structure. And for Cz-1TPE, two possible structure (**Figure 12C**) is exhibited as the two peaks of HPLC (27.8 min, 29.4 min) after photo-oxidation (**Figure 9A**). This small change in molecule structure makes it from AIE active molecule to ACQ molecule. These characteristics are supported by the strong enhanced emission in dilute solution and nearly quenching in thin film after UV irradiation. It should be noted that in solutions the concentration affects the conversion of photo-oxidation greatly. From the HPLC results of high concentration solution (10^{-3} M), we can observe that, upon 1 h UV irradiation, only very little photo oxidation products form (0.50 % at 27.8 min, 0.89% at 29.4 min). Even it is irradiated up to 3 h, the photo-oxidation reaction rate is still slow (1.42 % at 27.4 min, 2.52% at 29.4 min). While for 10^{-5} M, the photo-oxidation product improves from 11.08% (27.8 min), 20.57% (29.4 min) at 1 h,40.68% (27.8 min), 78.04% (29.4 min) at 2 h, to 47.85% (27.8 min), 73.54% (29.4 min) at 3 h. We propose that O_2 might participate in the photo-oxidation process. In dilute solutions, the amount of O_2 in solution could be treated as constant without changing the volume and temperature of the sample during photo-oxidation experiment. Consequently, in concentrated solutions the conversion is much lower compared with dilute solutions in same irradiation time.

It is interesting to note that the Cz-4TPE in solution shows very little changes until 3 h irradiation while Cz-1TPE exhibits strong emission in just 5 min, meanwhile the UV-Vis absorption of all the Cz-TPEs exhibit similar changes upon UV irradiation. We make the plot of I/I_0 (fluorescence intensity at 407 nm) and A/A_0 (the Abs at 335 nm for Cz-1TPE, 338 nm for Cz-2TPE, 338 nm for Cz-3TPE, 326 nm for Cz-4TPE, 360 nm for Cz-2TPE (2, 7)) with UV irradiation time (see **Figure 8F$_1$** and **8F$_2$**). We can see from **Figure 8F$_2$**, all the absorbance decreases gradually as we increasing the irradiation time, which indicates that the photo oxidation process happens uniformly for all the Cz-TPEs without exception. We suppose the difference in the numbers of TPE in the molecules is the main reason. When the only one TPE in Cz-1TPE is oxidized, the product will "soon" turn from AIE-active to ACQ; while as to Cz-4TPE, even one or two TPEs in the molecule are oxidized, it might still remain AIE-active and as a result the fluorescence changes much "slower" than that of Cz-1TPE. Generally, we can observe the fluorescence changes trends in Cz-1TPE＞Cz-2TPE≈Cz-2TPE (2, 7)＞Cz-3TPE＞Cz-4TPE from **Figure 8F$_1$**.

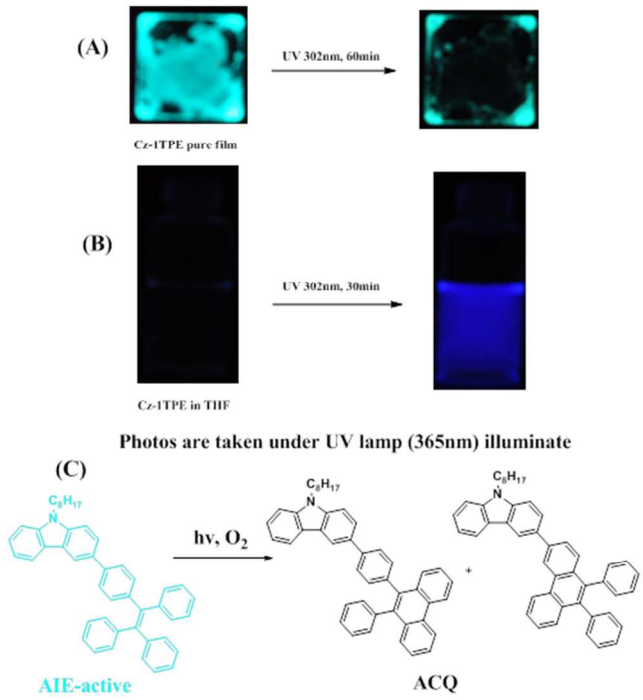

Figure 12 (A) Photos of Cz-1TPE in thin film before and after UV (302nm) irradiation (60 min), **(B)** Fluorescence images of Cz-1TPE in THF solution before and after UV (302 nm) irradiation (30 min) at UV (365nm) lamp excitation, **(C)** proposed mechanism during the photo-oxidation process of Cz-1TPE.

Similarly, the plot of I/I_0 (fluorescence intensity at 483nm) with different UV irradiation time to was made to investigate the photo oxidation in thin film (see **Figure 11F**). The I/I_0 value of Cz-1TPE decreases the slowest, while those of Cz-2TPE and Cz-3TPE are the fastest, which is quite different from that in THF. We suppose that "this disorder" in the fluorescence response to UV light irradiation might be attributed to the following reasons. In solid state, the concentration effect disappears instead by the thickness of the films. The prepared films by spin coating method could hardly be made with highly uniform, especially for small organic molecules, since the thickness of the film affects a lot to their fluorescence response to UV light. As a result, in film the fluorescence changes upon UV light irradiation looks "disorder" compared to that in THF. However, we can conclude that in thin film state all the Cz-TPEs could be photo oxidized by UV light from these results.

Theoretical calculations

To further understand the correlation between structure and the physical properties as well as the device performance, quantum chemistry computations were conducted. The geometries of the molecules have been optimized using DFT calculations with the B3LYP exchange-correlation functional and a 6-31g* basis set. **Figure 13** shows the optimized geometries and the orbital

distributions of HOMO and LUMO energy levels of Cz-TPEs (the HOMO and LUMO data is calculated from UV-Vis absorption and CV). The LUMO electron clouds of Cz-1TPE and Cz-2TPE are distributed at TPE groups (3 and/or 6 position), which is different from that of Cz-3TPE and Cz-4TPE (TPE at 1 and/or 8 position of carbazole).The LUMO level of Cz-2TPE (2, 7) is well-distributed in both TPE and carbazole, which might be because of the symmetry of the molecule and better conjugation at the 2 and 7 position of carbazole. The electron clouds of HOMO levels of all the Cz-TPEs are dominated by the carbazole and TPE at 3 and 6 position.

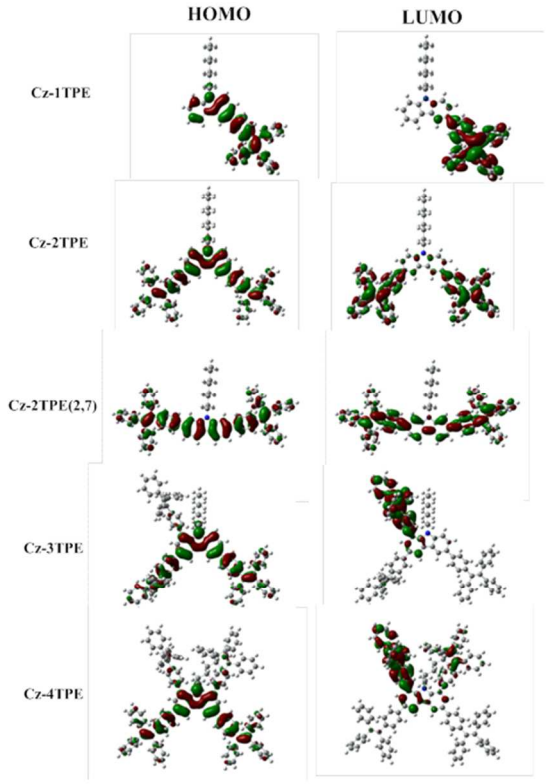

Figure 13 Calculated molecular orbital amplitude plots of HOMO and LUMO levels of Cz-TPEs and the energy levels calculated from CV and UV-Vis absorption.

Electrochemical and Electroluminescence properties

The electrochemical properties of Cz-TPEs were investigated by cyclic voltammetry (CV) (**Figure 14**). The HOMO energy levels were calculated to be 5.01 eV, 4.96 eV, 5.07 eV, 4.96 eV and 4.97 eV for Cz-1TPE, Cz-2TPE, Cz-3TPE, Cz-4TPE and Cz-2TPE (2, 7), respectively, according to the following equation: HOMO = - (4.8+ E_{ox}) eV. The single TPE molecule is also measured in the same way with a HOMO value of 5.69 eV. Their LUMOs could be obtained from optical band gap energies (estimated from the onset wavelength of their UV absorptions) and HOMO values, which gave LUMO values of 1.21 eV, 1.25 eV, 1.43 eV, 1.37 eV and 1.39 eV for Cz-1TPE, Cz-2TPE, Cz-3TPE, Cz-4TPE and Cz-2TPE (2, 7), respectively.

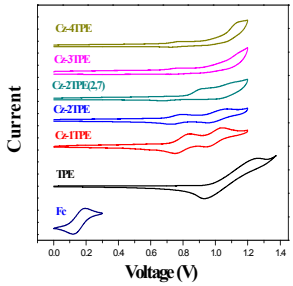

Figure 14 Cyclic voltammogram of Cz-1TPE, Cz-2TPE, Cz-2TPE (2, 7), Cz-3TPE, Cz-4TPE and TPE measured in distilled dichloromethane containing 0.1 M tetra-n-butyl-ammonium hexafluoro-phosphate. Scan rate: 100 mV /s.

After we have obtained the theory calculation and electrochemical properties of these Cz-TPEs, we fabricated multilayer OLED devices with configuration ITO/PEDOT (40 nm)/Cz-TPEs (50 nm)/TPBi (40 nm)/LiF (1 nm)/Al (100 nm) by spin coating deposition processes, in which Cz-TPE materials serves as the emitting layer, PEDOT functions as the hole-transporting layer and TPBi (1, 3, 5-tris(N-phenyl-benzimidazol-2-yl)benzene) functions both as the hole-blocking and electron transporting layer. The detail procedures are performed by dissolving 10 mg Cz-TPEs into 1 ml THF and this solution was then spin-coated at 1000 rad/s for 1 min. The thickness of the emitting layer was calculated to be ~50 nm. The EL spectra, current density–voltage–brightness (J–V–L) characteristics, efficiency versus current density curves, efficiency versus power efficiency, energy diagrams and device configurations are shown in **Figure 15**.

As shown in **Figure 15A**, the electroluminescence devices of Cz-TPEs exhibit similar characteristics compared to the PL spectra in thin film and the CIE coordinates are thus calculated to (0.18,0.34), (0.20,0.40), (0.20,0.39), (0.20,0.38) and (0.20,0.38) for Cz-1TPE, Cz-2TPE, Cz-3TPE, Cz-4TPE, Cz-2TPE (2, 7), respectively. The devices based on Cz-TPEs (with the same sequence) exhibit a maximum luminance (L_{max}) of 2858, 1353, 986, 2088 and 1129 cd m^{-2}, a maximum current efficiency ($\eta_{c,max}$) of 3.5, 4.9, 3.1, 3.1 and 5.5 cd A^{-1}, a maximum power efficiency ($\eta_{P,max}$) of 2.1, 3.9, 2.2, 1.8 and 3.1 lm W^{-1} and turn on voltage (V_{on}) 3.5, 3.5, 3.3, 3.6 and 4.2 V, respectively. The detailed EL performances are listed in **Table 2**.

We have previously reported a series of fluorene oligomer end capped TPE materials ($F_{(1\sim5)}$-TPE) and investigated its EL performances. With the same EL device structures and similar conditions, it is satisfied that the Cz-TPEs based EL devices exhibit great improvements compared to those of $F_{(1\sim5)}$-TPEs. Cz-1TPE exhibits the highest L_{max} with 2585 cd m^{-2}, which is 2 times of the F-1TPE (1300 cd m^{-2}, highest among $F_{(1\sim5)}$-TPE).The $\eta_{c,max}$, $\eta_{P,max}$ of Cz-TPEs are around 3.1-5.5 cd A^{-1} and 1.8-3.9 lm W^{-1}, while the highest for $F_{(1\sim5)}$-TPE are only 2.6 cd m^{-2} and 1.0 lm W^{-1}. All the Cz-TPEs show lower turn on voltage compared to those of $F_{(1\sim5)}$-TPE (4.8-6.4 V) with the lowest 3.3 V for the device of Cz-3TPE. The better matching of

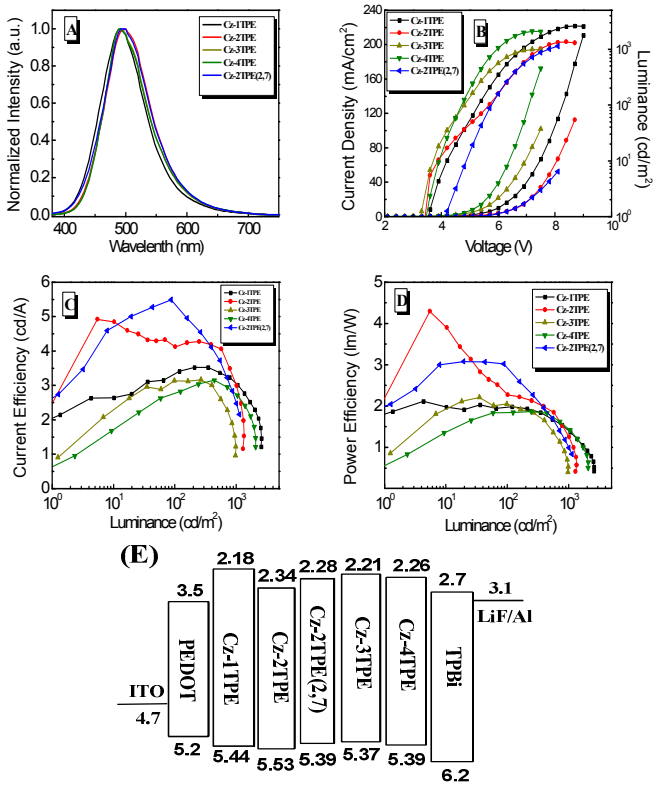

Figure 15 (**A**) EL spectra of Cz-1TPE, Cz-2TPE, Cz-3TPE, Cz-4TPE, Cz-2TPE (2, 7); (**B**) change in luminance and current density with the applied bias, (**C**) luminance versus current efficiency; (**D**) luminance versus power efficiency; (**E**) energy level diagrams and device configurations of multilayer EL devices of Cz-1TPE, Cz-2TPE, Cz-3TPE, Cz-4TPE, Cz-2TPE (2, 7), Device configurations: ITO/PEDOT (40 nm)/Cz-TPEs (50 nm) /TPBi (40 nm)/LiF (1 nm)/Al; Abbreviations: TPBi = 1, 3, 5-tris(N-phenyl-benzimidazol-2-yl)benzene.

HOMO energy level to PEDOT and good hole transporting properties of carbazole moieties might be the main reasons for the EL performance improvements.

Table 2 EL performances of Cz-TPEs[a]

Cz-TPE	λ_{EL} nm	V_{on} V	L_{max} cd m^{-2}	$\eta_{P,max}$ lmW^{-1}	$\eta_{c,max}$ cd A^{-1}	*CIE* (x,y)
1TPE	492	3.5	2585	2.1	3.5	(0.18, 0.34)
2TPE	500	3.5	1353	3.9	4.9	(0.20, 0.40)
3TPE	492	3.3	986	2.2	3.1	(0.20, 0.39)
4TPE	492	3.6	2088	1.8	3.1	(0.20, 0.38)
2TPE (2,7)	492	4.2	1129	3.1	5.5	(0.20, 0.38)

[a] Abbreviations: V_{on} = turn-on voltage at 1 cd m^{-2}, L_{max} = maximum luminance, $\eta_{P,max}$, and $\eta_{C,max}$ = maximum power and current efficiencies, respectively. *CIE* = Commission International de l'Eclairage coordinates.

Conclusions

In this paper, we design and synthesis a series of novel TPE-decorated carbazole fluorophores with aggregation-induced emission characteristics. The bromination of carbazole has been controlled and then the subsequent mono, di, tri and tetra-bromocarbazoles have been subjected to Suzuki cross-coupling to yield a series of carbazole-tetraphenylethene (TPE) materials with varying the number of peripheral TPE groups. We have carried out a comparative study of their thermal, optical, electrochemical and electroluminescence properties.

From the DSC and TGA curves, the glass transition temperature increases as the number of tetraphenylethene groups increases around the central carbazole ring (20.7°C to 137.5°C) and all oligomers exhibit good thermal stability with high thermal decomposition temperatures in the range of 331°C to 493°C. Generally, the molar absorptivity (ε) of Cz-TPEs increases as there are more TPE groups connecting to carbazole and the substitution at 2, 7 positions contributes more to the conjugation of the whole molecule compared to others at 1,3,6,8 positions of carbazole.

All the Cz-TPEs are non-fluorescent in THF and emit strong blue-green fluorescence in thin film because of their AIE nature. In the water-THF measurements, the emission starts to light up "earlier" with lower water content (f_w) when there are more TPEs in the molecules, which could be attributed to the fact that more TPEs in the molecules make it more insoluble in water and thus the rotation of the phenyls in TPE becomes much easier to be restricted in the poor solvent mixtures.

In THF (10^{-5} M) solution, all the Cz-TPEs emit deep blue light after proper time of UV (302 nm) irradiation and we find that the more TPE groups, the slower the fluorescence enhances. In thin film (40 nm), the emission maximum blue shift, decreases and finally becomes non-emissive after about 1.5 h for all the Cz-TPEs. We suppose these optical properties are attributed to the photo induced irreversible changes of TPE to diphenylphenanthrene derivatives. The photo oxidation process of Cz-1TPE in solution is also investigated and proved by HPLC analysis, ^{1}H NMR and LC-MS.

Consequently, we applied the Cz-TPEs to OLED devices by spin coating deposition process with OLED devices configuration: ITO/PEDOT (40 nm)/Cz-TPEs (50 nm)/TPBi (40nm)/LiF (1 nm)/Al (100 nm). All the EL devices emit blue-green light with a maximum luminance (L_{max}) of 2858, 1353, 986, 2088 and 1129 cd m^{-2}, a maximum current efficiency ($\eta_{c,max}$) of 3.5, 4.9, 3.1, 3.1 and 5.5 cd A^{-1}, a maximum power efficiency ($\eta_{P,max}$) of 2.1, 3.9, 2.2, 1.8 and 3.1 lm W^{-1} and turn on voltage (V_{on}) 3.5, 3.5, 3.3, 3.6 and 4.2 V, for Cz-1TPE, Cz-2TPE, Cz-3TPE, Cz-4TPE, Cz-2TPE (2, 7), respectively

The photo oxidation of Cz-TPEs is a common phenomenon in both solution and thin films regardless of the number of the TPEs or substitute positions at the carbazole from our work. It is worthwhile to note that the photo oxidation in dilute solutions (10^{-5}M) and thin films (thickness ~40nm) upon UV (302nm) light irradiation are rather obvious. As the sustained growing and increasing passion of investigation in TPE molecules in recent years, designing more photo stable TPE molecules might be an important research topic. Our group has been undertaken synthesizing modified TPEs to achieve this goal.

Acknowledgements

This work was supported by the NSFC (20874025, 21174045), National Basic Research Program of China (Grant No.2013CB922104). M.P.A. acknowledges the NSFC Research Fellowship for International Young Scientists (21150110141, 212111128). M.Q.Z. acknowledges the Open Program for Beijing National Laboratory for Molecular Sciences (BNLMS). We also thank Analytical and Testing Center of Huazhong University of Science and Technology.

Notes and references

[a] Wuhan National Laboratory for Optoelectronics, School of Optical and Electronic Information, Huazhong University of Science and Technology, Wuhan, Hubei, China, 430074. Fax: (+86)027- 8779341. E-mail: mqzhu@hust.edu.cn.

Electronic Supplementary Information (ESI) available: synthetic procedures and characterization. See DOI: 10.1039/b000000x/

1 Citations here in the format A. Name, B. Name and C. Name, *Journal Title*, 2000, **35**, 3523; A. Name, B. Name and C. Name, *Journal Title*, 2000, **35**, 3523.

1 For selected papers (a) X. Zhu, J. Peng, Y. Cao and J. Roncali, *Chem. Soc. Rev.* 2011, **40**, 3509-3524; (b) Y. Shirota, *J. Mater. Chem.* 2000, **10**, 1-25; (c) L. Yao, S. Xue, Q. Wang, W. Dong, W. Yang, H. Wu, M. Zhang, B. Yang and Y. Ma, *Chem. Eur. J.* 2012, **18**, 2707-2714; (d) K. Brunner, A. van Dijken, H. Borner, J. Bastiaansen, N. Kiggen and B. Langeveld *J. Am. Chem.* Soc. 2004, **126**, 6035-6042.

2 K.-Y. Law, *Chem. Rev.* 1993, **93**, 449-486

3 (a) J. Li and A. Grimsdale, *Chem. Soc. Rev.* 2010, **39**, 2399-2410; (b) J. Tang, J. Hua, W. Wu, J. Li, Z. Jin, Y. Long and H. Tian, *Energy Environ. Sci.* 2010, **3**, 1736-1745; (c) M. Liang and J. Chen, *Chem. Soc. Rev.* 2013, **42**, 3453-3488; (d) D. Gendron and M. Leclerc, *Energy Environ. Sci.* 2011, **4**, 1225-1237

4 (a) X. Zhao, Z. Zhang, Y. Qian, M. Yi, L.i Xie, C. Hu, G. Xie, H. Xu, C. Han, Y. Zhao, W. Huang, *J. Mater. Chem. C*. 2013, **1**, 3482-3490; (b) J. Li, D. Liu, Y. Li, C. Lee, H. Kwong, and S. Lee, *Chem. Mater.*2005, **17**, 1208-1212; (c) M. Park and J. Lee, *Chem. Mater.* 2011, **23**, 4338-4343; (d) K. Thomas, J.Lin, Y.Tao, and C. Ko, *J. Am. Chem. Soc.* 2001, **123**, 9404-9411.

5 (a) Y. Tao, C. Yang, J. Qin, *Chem. Soc. Rev.* 2011, **40**, 2943-2970; (b) K.Yook and J. Lee, *Adv. Mater.* 2012, **24**, 3169-3190, (c) L. Cui, S. Dong, Y. Liu, Q. Li, Z. Jiang, L. Liao, *J. Mater. Chem. C*. 2013, **1**, 3967-3975.

6 (a) O. Paliulis, J. Ostrauskaite, V. Gaidelis, V.Jankauskas and P. Strohriegl, *Macromol. Chem. Phys.* 2003, **204**, 1706; (b) M. Sonntag and P. Strohriegl, *Chem. Mater.* 2004, **16**, 4736.

7 (a) W. Gong, F. Zhong, M. Aldred, Q. Fu, T. Chen, D. Huang, Y. Shen, X. Qiao, D. Ma and M. Zhu, *RSC Adv*. 2012, **2**, 10821-10828; (b) M. Aldred, C. Li, G. Zhang, W. Gong, A.D.Q. Li, D. Feng, D. Ma and M. Zhu, *J. Mater. Chem.* 2012, **22**, 7515-7528.

8 Y. Hong, J. W. Y. Lam and B. Tang, *Chem. Soc. Rev.* 2011, **40**, 5361-5388.

9 J. Luo, Z. Xie, J. W. Y. Lam, L. Cheng, H. Chen, C. Qiu, H. Kwok, X. Zhan, Y. Liu, D. Zhu and B. Tang, *Chem. Comm.* 1740-1741.

10 (a) M. Han and M. Hara, *J. Am. Chem. Soc.* 2005, **127**, 10951; (b) Y. Li, F. Li, H. Zhang, Z. Xie, W. Xie, H. Xu, B. Li, F. Shen, L. Ye, M. Hanif, D. Ma and Y. Ma, *Chem. Commun.* 2007, 231-233; (c) N. S. S. Kumar, S. Varghese, N. P. Rath, and S. Das, *J. Phys. Chem. C* 2008, **112**, 8429-8437; (d) R. Davis, N. S. S. Kumar, S. Abraham, C. H. Suresh, N. P. Rath, N. Tamaoki, and S. Das, *J. Phys. Chem. C* 2008, **112**, 2137-2146; (e) R. Davis, N. P. Rath and S. Das, *Chem. Commun.* 2004, 74-75; (f) Y. Zhang, G. Zhuang, M. Ouyang, B. Hu, Q. Song, J. Sun, C. Zhang, C. Gu, Y. Xu, Y. Ma, *Dyes and Pigments* 2013, **98**, 486-492; (g) Y. Zhang, J. Sun, X. Lv, M. Ouyang, F. Cao, G. Pan, L. Pan, G. Fan, W. Yu, C. He, S. Zheng, F. Zhang, W. Wang and C. Zhang, *Cryst. Eng. Comm.* 2013, **15**, 8998-9002.

11 (a) H. C. Yeh, W. C. Wu, Y. S. Wen, D. C. Dai, J. K. Wang and C. T. Chen, *J. Org. Chem.* 2004, **69**, 6455; (b) S. S. Palayangoda, X. Cai, R. M. Adhikari and D. C. Neckers, *Org. Lett.* 2008, **10**, 281.

12 Z. Wang, H. Shao, J. Ye, L. Tang, and P. Lu, *J. Phys. Chem. B* 2005, **109**, 19627-19633.

13 K.Kokado and Y. Chujo, *Macromolecules* 2009, **42**, 1418.

14 H. Lu, B. Xu, Y. Dong, F. Chen, Y. Li, Z. Li, J. He, H. Li, and W. Tian, *Langmuir* 2010, **26**, 6838-6844

15 X. Shi, H. Wang, T. Han, X. Feng, B. Tong, J. Shi, J. Zhi and Y. Dong, *J. Mater. Chem.* 2012, **22**, 19296-19302.

16 (a) M. Zhu, G. Zhang, Z.Hu, M. Aldred, C. Li, W. Gong, T. Chen, Z. Huang, S. Liu. *Macromolecules* 2014, **47**, 324-332. (b) M. Zhu, T. Chen, G. Zhang, C. Li, W. Gong, Z. Chen, M. Aldred. *Chem. Commun*. 2014, **50**, 2664-2666.

17 Y. You, H. S. Huh, K. S. Kim, S.W. Lee, D. Kim and S. Y. Park, *Chem. Commun.* 2008, 3998.

18 R. Hu, N. Leung and B. Tang, *Chem. Soc. Rev.* **DOI:** 10.1039/C4CS00044G.

19 (a) Z. Zhao, J. W. Y. Lam and B. Tang, *J. Mater. Chem.* 2012, **22**, 23726; (b) S. Chen, J. Liu, Y. Liu, H. Su, Y. Hong, C. K. W. Jim, R. T. K. Kwok, N. Zhao, W. Qin, J. Lam, K. Wong and B. Tang, *Chem. Sci.* 2012, **3**, 1804-1809.

20 W.-L. Gong, M. P. Aldred, G.-F. Zhang, C. Li and M.-Q. Zhu, *J. Mater. Chem. C* 2013, **1**, 7519-7525.

21 (a) Z. Zhao, C. Chan, S. Chen, C. Deng, J. Lam, C.Jim, Y. Hong, P. Lu, Z. Chang, X.g Chen, P. Lu, H. Kwok, H. Qiu and B. Tang, *J. Mater. Chem.* 2012, **22**, 4527–4534; (b) J. Huang, X. Yang, J. Wang, C. Zhong, L. Wang, J. Qin and Z. Li, *J. Mater. Chem.* 2012, **22**, 2478-2484; (c) Z. Zhao, J. Lam, C. Chan, S. Chen, J. Liu, P. Lu, M. Rodriguez, J. Maldonado, G. Ortiz, H. Sung, I. Williams, H. Su, K. Wong, Y. Ma, H. Kwok, H. Qiu, and B. Tang, *Adv. Mater.* 2011, **23**, 5430-5435; (d) Z. Yang, Z. Chi, T. Yu, X. Zhang, M. Chen, B. Xu, S. Liu, Y. Zhang and J. Xu, *J. Mater. Chem.* 2009, **19**, 5541-5546; (e) S. Odabas, E. Tekin, F. Turksoy and C. Tanyeli, *J. Mater. Chem. C* 2013, **1**, 7081-7091.

22 Z. Yang, Z. Chi, B. Xu, H. Li, X. Zhang, X. Li, S. Liu, Y. Zhang and J. Xu, *J. Mater. Chem.* 2010, **20**, 7352-7359.

23 W. Wu, S. Ye, L. Huang, L. Xiao, Y. Fu, Q. Huang, G. Yu, Y. Liu, J. Qin, Q. Li and Z. Li, *J. Mater. Chem.* 2012, **22**, 6374-6382.

24 (a) M. P. Aldred, C. Li, and M.-Q. Zhu, *Chem. Eur. J.* 2012, **18**, 16037-16045; (b) B. Jiang, D. Guo, Y. Liu, K. Wang and Y. Liu, *ACS Nano* 2011, **2**, 1609-1618; (c) G. Huang, B. Ma, J. Chen, Q. Peng, G. Zhang, Q. Fan, and D. Zhang, *Chem. Eur. J.* 2012, **18**, 3886-3892; (d) C. E. Bunker, N. B. Hamilton, and Y.-P. Sun, *Anal. Chem.* 1993, **65**, 3460-3465.

Tetraphenylethene-Decorated Carbazoles: Synthesis, Optical Properties, Aggregation Induced Emission and Photooxidation

Wen-Liang Gong, Matthew. P. Aldred,* Chong Li, Guo-Feng Zhang, Tao Chen, and Ming-Qiang Zhu*

Table of Content image and text

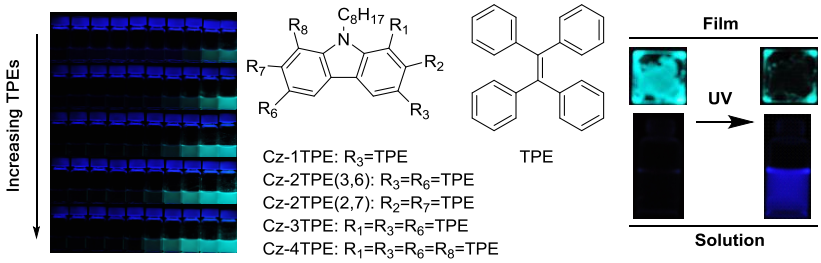

Five tetraphenylethene-decorated carbazoles with substitution at 1,3,6,8-positions of carbazole (Cz-1TPE, Cz-2TPE, Cz-3TPE and Cz-4TPE) are synthesized. They are non-fluorescent in THF and emit strong blue-green fluorescence in thin film because of their aggregation induced emission (AIE) nature while strong emission in THF and strong fluorescence quenching in thin film are observed upon UV irradiation.